

RSC Advances



This is an *Accepted Manuscript*, which has been through the Royal Society of Chemistry peer review process and has been accepted for publication.

Accepted Manuscripts are published online shortly after acceptance, before technical editing, formatting and proof reading. Using this free service, authors can make their results available to the community, in citable form, before we publish the edited article. This *Accepted Manuscript* will be replaced by the edited, formatted and paginated article as soon as this is available.

You can find more information about *Accepted Manuscripts* in the [Information for Authors](#).

Please note that technical editing may introduce minor changes to the text and/or graphics, which may alter content. The journal's standard [Terms & Conditions](#) and the [Ethical guidelines](#) still apply. In no event shall the Royal Society of Chemistry be held responsible for any errors or omissions in this *Accepted Manuscript* or any consequences arising from the use of any information it contains.

Design and Preparation of Bio-based Dielectric Elastomer with Polar and Plasticized Side Chains

Weiwei Lei,^a Runguo Wang,^a Dan Yang,^d Guanyi Hou,^a Xinxin Zhou,^a He Qiao,^a
Wencai Wang,^a Ming Tian,^a Liqun Zhang^{*abc}

^aState Key Laboratory for Organic–Inorganic Composites, Beijing University of Chemical Technology, Beijing 100029, China.

E-mail: zhanglq@mail.buct.edu.cn; Fax: +86-10-64456158; Tel: +86-10-64443413

^bKey Laboratory of Beijing City for Preparation and Processing of Novel Polymer Materials, Beijing University of Chemical Technology, Beijing 100029, China.

^cBeijing Engineering Research Center of Advanced Elastomers, Beijing University of Chemical Technology, Beijing 100029, China.

^dBeijing Key Lab of Special Elastomer Composite Materials, Beijing Institute of Petrochemical Technology, Beijing 102617, China

Abstract

A new dielectric elastomer with large actuated strain driven by low electric field was synthesized from di-*n*-butyl itaconate and isoprene through free radical redox emulsion polymerization. The effect of the copolymerized proportion of poly(di-*n*-butyl itaconate-*co*-isoprene) (PDBII) and the dosage of crosslinking agent on the elastic modulus, dielectric properties, and actuated strain of the elastomer were investigated, and a potential dielectric elastomer candidate containing 70 wt % di-*n*-butyl itaconate was obtained. The permittivity of the PDBII crosslinked by 3.0

phr of dicumyl peroxide was 5.68 at 10^3 Hz, which was higher than that of commercial acrylic and silicone dielectric elastomers. Without any prestrain, an actuated strain of 20% was obtained at an electric field of 30 kV mm^{-1} . In order to further increase the actuated strain, barium titanate (BaTiO_3), a high-dielectric-constant ceramic powder, was utilized to fill the PDBII to form a BaTiO_3 /PDBII composite. The dielectric constant of the composite increased with increasing content of BaTiO_3 , and the elastic modulus of the composite was lower than that of the unfilled PDBII, leading to a larger dielectric actuated strain of the composite.

Introduction

Dielectric elastomer is a kind of intelligent multifunctional electroactive polymer. Dielectric elastomers offering performance such as large active strain, fast response, high electromechanical coupling efficiency, light weight, freedom from noise, and low cost^{1, 2} have drawn significant interest in recent years, especially after silicone and acrylic elastomer films with strains in excess of 100% have been reported.^{3, 4} Several applications have already been developed, including artificial muscles,⁵ sensors,⁶ micro air vehicles,⁷ and electrical power generator⁸.

A dielectric elastomer actuator consists of a thin film sandwiched between two compliant electrodes.⁹ When an electric field is applied, an electrostatic pressure acts on the film, shrinking in the thickness direction and elongating in the planar direction. The actuated strain in the thickness direction is given by the following equation:

$$s_z = p/Y = \frac{\epsilon\epsilon_0}{Y} \left(\frac{U}{d}\right)^2 \quad (1)$$

where p is the electrostatic pressure, Y is the elastic modulus, ε is the permittivity of the elastomer, ε_0 is the permittivity of free space, U is the applied voltage, and d is the thickness of the film.³ Elastomers with high dielectric constant and low elastic modulus are interesting candidates for dielectric using. A large number of elastomers were tested, including silicone,¹⁰ fluoroelastomer⁵, acrylic elastomer¹¹ and some kind of thermoplastic elastomers¹¹. However, none of these materials were developed for actuator applications because excessively high operation voltages would be required, causing security risk and increasing the costs of devices. Great efforts have been made to develop new materials that can be activated at low voltages.

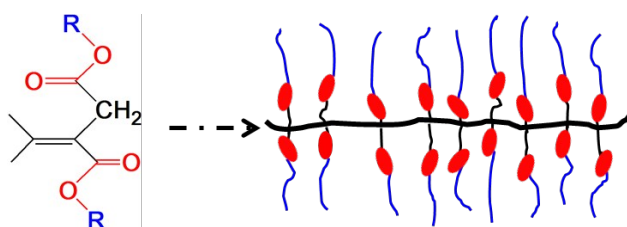
Most studies have focused on the development of high permittivity polymer composites by loading the elastomer matrix with insulating or conductive fillers. The most commonly followed approach utilized high permittivity ceramic fillers in the form of powder, such as barium titanate,¹² lead-magnesium niobate,¹³ and titanium dioxide^{14, 15}. Usually the dielectric improvement needs a high ceramic filler content, which would increase the elastic modulus. Another approach was to prepare percolative composites utilising conductive fillers such as metal nanoparticles,¹⁶ polyaniline,¹⁷ carbon nanotubes,^{18, 19} and graphite nanoplates²⁰. The permittivity can dramatically increase as the content of conductive filler approaches the percolation threshold, i.e., less than 20% for a microcapacitor network in a composite. Such percolative composites generally have high dielectric losses near the percolation threshold, mainly because large leakage currents are generated between the connecting conductive fillers. Efforts to modify the fillers to improve the dielectric

performance of elastomer composites include the surface modification of BaTiO₃²¹⁻²³ and titanium dioxide (TiO₂)²⁴ to get a homogeneous dispersion and the coating of conductive fillers with an insulating layer to avoid the direct contact of conductive fillers with one another. Another way to increase the actuated strain and the dielectric strength of dielectric elastomer is the application of high prestrain,³ which will reduce the thickness of the dielectric elastomer and lead to the alignment of macromolecule chains perpendicular to the applied electric field. However, a rigid frame or supporting structure was needed to maintain the structure of the dielectric film,²⁵ and the stress relaxation and fatigue of the film after prestraining will take place as time goes by. Previous studies mostly focused on the filler and ignored the matrix, but the matrix was also critical for an excellent dielectric elastomer composite to have a low elastic modulus and high dielectric constant. Despite a great many of dielectric elastomer composites have been developed, there was still a severe lack of elastomer with a favorable profile of mechanical and dielectric properties.

The aim of this study was to design and prepare a novel dielectric elastomer based on di-*n*-alkyl itaconate. Di-*n*-alkyl itaconic acid ester can be readily polymerized to form a comb-branched structure, which was an excellent candidate for the investigation of ordering in amorphous structures. Nanophase separation of the incompatible main chains and side chains of poly(di-*n*-alkyl itaconates) has been extensively studied by differential scanning calorimetry (DSC),²⁶ dynamic mechanical analysis (DMA),^{27, 28} dielectric spectroscopy,²⁹ nuclear magnetic resonance (NMR),^{30, 31} and molecular modeling,³¹ leading to a deeper understanding of the relative roles of

intramolecular constraints and intermolecular interactions in the solid-state organization and properties of these polymers. The dielectric elastomers based on di-*n*-alkyl itaconate are readily polarized, and the alkyl groups provide the nanoheterogeneity and the plasticizing effect^{29,31,32}. The structure of PDBII is shown in Scheme 1, this structure is similar to that of acrylic elastomer.

Scheme 1. Synthesis of Dielectric Elastomer with Easily Polarized Ester Groups (red circles) and Flexible Alkyl Groups (blue lines) From Itaconate.



Itaconic acid, which has been categorized as one of the “top 12” building block molecules in advanced biorefineries³³, is a monomer obtained at low cost from renewable resources by fermentation. Butanol and isoprene were used in synthesize PDBII together with itaconic acid. Butanol was used because it has the appropriate side chain length to polymerize a low glass transition temperatures polymer and it is a high-efficiency, renewable biofuel. The isoprene will soften the polymer and provide the crosslinking points. Bio-based isoprene has aroused considerable interest and it is already available in the market. A free radical redox emulsion polymerization method^{34,35} was used to synthesize PDBII, as we did our previous work³⁴. The molar ratio of itaconate to isoprene, crosslinking agent dosage, and the content of the high-dielectric ceramic BaTiO₃ were studied to modulate the electromechanical properties.

Experimental

Materials

Itaconic acid (purity of 99%) was purchased from Qingdao Langyatai Group Co., Ltd. Butanol (purity of 97%) was purchased from Sigma-Aldrich Company. Isoprene (purity of 95%) was purchased from Alfa Aesar Company and distilled to remove any stabilizer before use. Ferric ethylenediaminetetraacetic acid salt (Fe(II) EDTA), sodium dodecyl benzene sulfonate (SDBS), sodium hydroxymethane sulfonate (SHS), tert-butyl hydroperoxide (TBH), potassium phosphate tribasic, potassium chloride, and hydroxylamine were purchased from Sigma-Aldrich Company and used as received without further purification. The crosslinking agent dicumyl peroxide (DCP) was purchased from Beijing Chemical Reagents Co., Ltd., China. BaTiO₃ nanoparticles (average particle size 30 nm) were purchased from Sigma-Aldrich Company. All the other agents were commercial products without further purification.

Methods

Synthesis of di-*n*-butyl itaconate (DBI)

Preparation of di-*n*-butyl itaconate monomer. Into a 1-L, three-neck glass flask equipped with a condenser, a thermometer, a mechanical agitator, and a Dean-Stark decanter, 130.1 g of itaconic acid, 160 ml of butanol, and 39.0 g of cyclohexane were added. After the mixture was heated to 115-130 °C, 1.38 g of sulfuric acid was added as catalyst. The reaction was considered complete when the quantity of byproduct (i.e.,

water) reached approximately 36.0 ml. The product was washed by deionized water in a separating funnel and distilled in vacuum to obtain di-*n*-butyl itaconate.

Synthesis of PDBII by redox-initiated free radical emulsion polymerization

The polymerization reactor was a 1-L, four-neck glass flask equipped with a reflux condenser, a sampling device, a nitrogen inlet, and a two-bladed anchor-type impeller. According to the formulation in Table 1, deionized water, SDBS, potassium phosphate tribasic solution, potassium chloride solution, Fe(II) EDTA solution, and SHS solution were added into the flask under high-speed stirring (400 rpm). Subsequently, pre-blended di-*n*-butyl itaconate and isoprene were added into the flask. A stable and homogeneous latex was obtained after 45 min of stirring. Later, TBH solution was injected into the flask and the stirring speed reduced to 200 rpm. The polymerization was allowed to proceed at 20 °C for 18 h to form the target PDBII latex, and hydroxylamine solution was added to terminate the reaction. The PDBII latex was coagulated by using an excess of calcium chloride solution. The wet product was washed with ethyl alcohol and water for five times and dried at 60 °C in vacuum until a constant weight was obtained.

Table 1. Formulation for redox-initiated emulsion polymerization

Ingredients (concentration)	Amount (g)
di- <i>n</i> -butyl itaconate	variable ^a
isoprene	variable ^a
deionized water	30% solid content
SDBS solution (10%)	5% weight of monomers
potassium phosphate tribasic solution (10%)	2
potassium chloride (10%)	5
SHS solution (10%)	2
Fe(II)EDTA solution (1%)	4

TBH solution (10%)	0.5
hydroxylamine solution (50%)	0.4

^adi-*n*-butyl itaconate and isoprene were copolymerized in mass ratios of 70/30 (PDBII-70), 50/50 (PDBII-50), and 30/70 (PDBII-30). Polyisoprene was also synthesized for comparison.

Preparation of cured PDBII and BaTiO₃/PDBII composites

The uncured PDBII was mixed with the crosslink agent DCP and the filler on a 6-in two-roll mill. The filled PDBII was cured at a pressure of 15 MPa for its optimum cure time at 165°C as determined by a disk oscillating rheometer (P3555B2, Beijing Huanfeng Chemical Machinery Experimental Factory, China). Recipe 1 contained 2.5 phr (parts per hundred of rubber) of DCP and 100 phr of PDBII-70, PDBII-50, or PDBII-30; recipe 2 contained 100 phr of PDBII-70 and different contents of DCP (0.5, 1.0, 1.5, 2.0, 3.0, 4.0, 5.0, and 6.0 phr); recipe 3 contained 100 phr of PDBII-70, 5 phr of DCP, and different contents of BaTiO₃ (0, 10, 30, 50, 70, and 90 phr).

Measurements

FTIR spectroscopy

The FTIR spectra of raw PDBII rubber were recorded on a Bruker Tensor 27 spectrometer (Bruker, Germany) to determine the structure of PDBII. The samples were prepared by cutting raw PDBII rubber into pieces. The spectra were obtained between 4000 and 400 cm⁻¹ at a resolution of 4 cm⁻¹ and over 32 scans.

¹H-NMR spectroscopy

The $^1\text{H-NMR}$ spectra of elastomers were recorded with a Bruker AV400 NMR spectrometer (Bruker, Germany) to determine the chemical structural of PDBII and polyisoprene at a frequency of 400 MHz and with CDCl_3 as solvent.

Gel permeation chromatography (GPC)

The molecular weight and polydispersity of PDBII were determined by gel permeation chromatography analysis on a Perkin-Elmer 200 gel permeation chromatography instrument with a PL mixed-B10m column and a reflective index detector. Tetrahydrofuran at a flow rate of 1.0 ml min^{-1} and $25 \text{ }^\circ\text{C}$ was used as the eluent, and the calibration was carried out with polystyrene standards.

Differential scanning calorimetry (DSC)

The thermal properties of pure PDBII were determined by using a Perkin-Elmer Pyris 1 series differential scanning calorimeter. The temperature was calibrated with indium and zinc, and the heat flow was calibrated with indium. A small section of a film was cut and weighed to 2-5 mg by using a Perkin-Elmer microbalance and sealed in crimped aluminum pan. The sample was heated from 25 to 150°C at a rate of $10^\circ\text{C min}^{-1}$ and cooled from 150°C to -100°C at a rate of $-20^\circ\text{C min}^{-1}$ under a nitrogen purge at a flow rate of 20 ml min^{-1} . The glass transition temperature was determined from the heating curve from -100 to 100°C at a rate of $10^\circ\text{C min}^{-1}$. A baseline was recorded with matching empty pan. Certified indium and sapphire were used for temperature and heat flow calibration.

Tensile properties

Tensile tests were performed on dumbbell-shaped samples (original length 25 mm) according to ASTM D412 by using a CMT 4104 electrical tensile apparatus (Shenzhen SANS Test Machine Co., Ltd., China) at a crosshead speed of 50 mm min⁻¹ and 25°C. The elastic modulus of a sample was determined from the slope of the stress-strain curve at 5% strain.

Dielectric analysis

The dielectric properties of the samples were measured with an impedance analyzer (E4980A, Agilent, USA) over the frequency range of 10 to 10⁶ Hz under a voltage of 1 V at room temperature.

Electric actuation tests

The samples for actuated strain tests were 0.4 mm thick. The compliant electrodes were fabricated by spraying with an airbrush a graphite suspension composed of graphite, silicone oil, and a crosslinking agent on the two surfaces of a dielectric elastomer film fixed on a circular frame. The strain was defined as the number of pixels (A) of the electrodes' area divided by the number of pixels before being applied voltage (A_0). The voltage was supplied by a high-voltage direct current generator (DTZH-60, Wuhan Dotek Electric Co., Ltd., China). A video camera was used at constant focal length to capture the actuator plane before and after the voltage was applied, and then the captured video pictures were processed with Photoshop software to determine the change in the number of pixels on the electrodes. The planar strain can be calculated by

$$S_p = (A - A_0)/A_0 \times 100\% \quad (1)$$

where A is the actuated planar area and A_0 is the original area. As it is difficult to accurately measure the change in thickness, we instead measured the change in planar area S_p to evaluate the thickness actuated strain S_z .

Based on the law of volume constancy,

$$(1 + S_p)(1 + S_z) = 1 \quad (2)$$

Rearrangement of eq(2) gives an expression for the planar strain:

$$S_p = \frac{1}{1+S_z} - 1 \quad (3)$$

According to eq(1),

$$S_p = \varepsilon_r \varepsilon_0 U / (dY - \varepsilon_r \varepsilon_0 U) \quad (4)$$

Every experimental data point of mechanical properties, dielectric properties, and electromechanical strain in this work was the average of the results obtained from at least five samples under the same conditions.

Results and discussion

Synthesis and Structure of Di-*n*-butyl Itaconate

Itaconic acid was capped with butanol, a renewable monomer, to restrain the chain the chain transfer effect of carboxyl groups. In Figure S1, the resonances at 5.69 and 6.32 ppm are both assigned to the C=CH₂ protons of itaconate, indicative of double bonds for subsequent reaction. Absorptions at 4.17, 4.10, 1.63, 1.61, 1.40 and 1.38 ppm are due to the d, e, f, g, h, i protons of the methylenes groups of the capped product, respectively. The absorptions at 0.95 and 0.93 ppm belong to the -CH₃

protons of butyl units. In conclusion, di-*n*-butyl itaconate was successfully produced.

Molecular weight and structural characteristics of PDBII

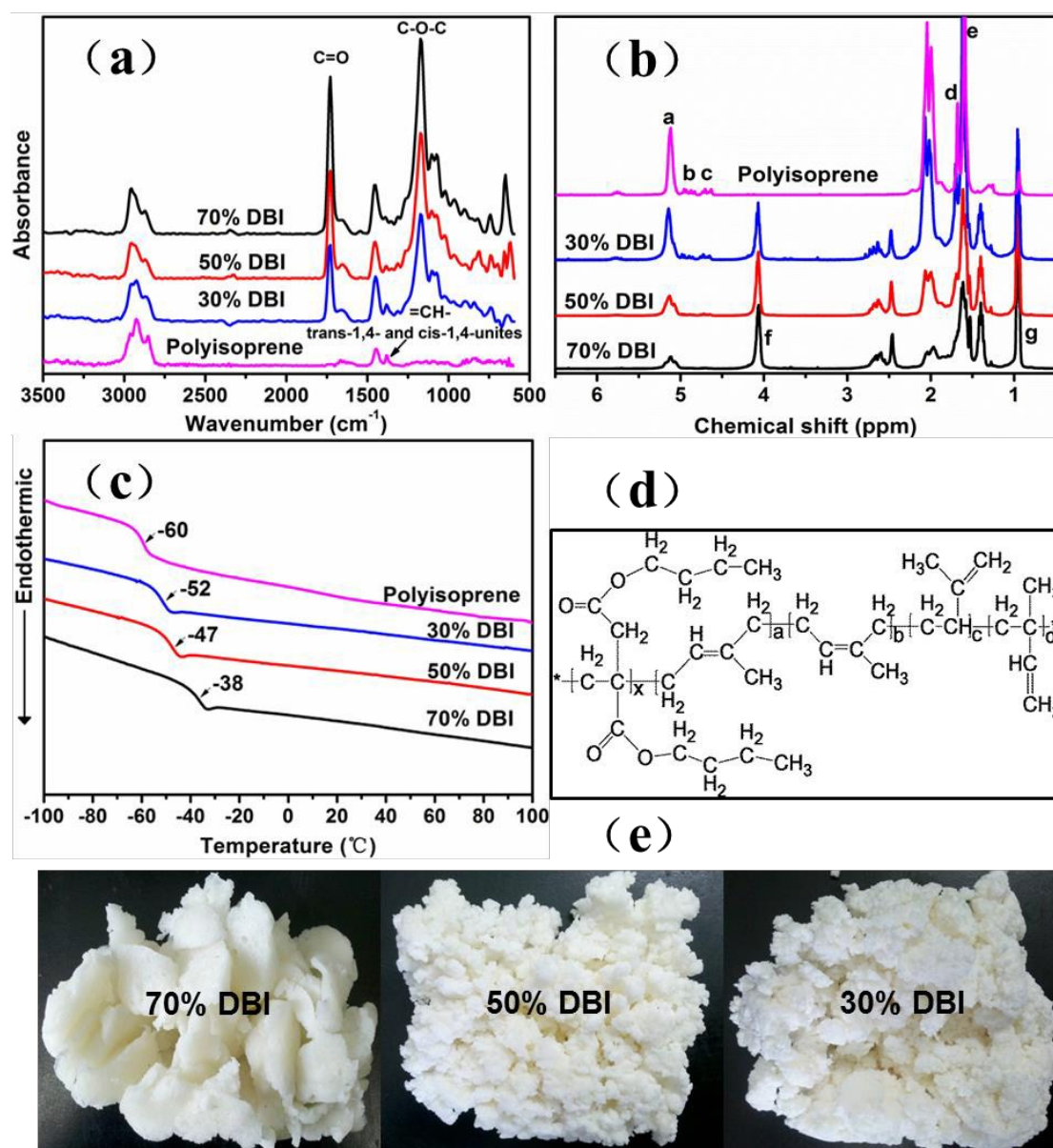


Figure 1. Samples of PDBII with different itaconate to isoprene feed ratios: (a) FTIR spectra, (b)

$^1\text{H-NMR}$ spectra, (c) DSC thermograms, (d) chemical structure, and (e) sample pictures (DBI:

di-*n*-butyl itaconate, i.e., 30% DBI means 30 wt % DBI in the feed).

The PDBIIs with different di-*n*-butyl itaconate content were synthesized, and Figure 1(e) shows photographs of the dry PDBIIs. As the isoprene content increased, the

polymer became less consolidated and soft. The GPC results listed in Figure S2 showed three traces with broad single peaks suggesting only one component exists. The number-average molecular weight of PDBII-70, PDBII-50, PDBII-30 were 19.3×10^4 , 18.1×10^4 , and 12.3×10^4 respectively, ensuring a sufficiently high elasticity for PDBII to be used as elastomers after being crosslinked.

As shown in Figure 1(a), although the most of the absorbance peaks of polyisoprene are overlapping, the peak at 1380 cm^{-1} representing the trans-1,4- and the cis-1,4-units of isoprene in the main chain can still be distinguished, and the intensity decreases as the di-n-butyl itaconate (DBI) content increases from 30% to 70%. The peak at 1730 cm^{-1} representing the carbonyl moieties (C=O) and the peak at 1170 cm^{-1} representing the asymmetric vibration of C-O-C indicate that DBI has been successfully copolymerized. Because most of the CH_3 and CH_2 absorption peaks are overlapping, the detailed structure of PDBII, in particular the copolymerization ratio, should be confirmed by $^1\text{H-NMR}$.

In Figure 1(b), the polyisoprene proton signals at 5.12 ppm ($=\text{CH}$ -, peak a), 4.88 ppm ($=\text{CH}_2$, peak b), and 4.67 ppm ($=\text{CH}_2$, peak c) represent the 1,4-units, 1,2-units, and 3,4-units, respectively. The peak areas indicate that the polyisoprene prepared by redox emulsion polymerization consists of 93% 1,4-units, 3.3% 1,2-units, and 3.7% 3,4-units. The area under peak e (1.59 ppm, $-\text{CH}_3$) is larger than that under peak d (1.68 ppm, $-\text{CH}_3$) because there are more trans-1,4-units than cis-1,4-units. The sharp peak g (0.92 ppm, $-\text{CH}_3$) corresponds to the $-\text{CH}_3$ in the DBI unit. From the areas under peaks g and a, we can deduce that PDBII-70, PDBII-50, and PDBII-30 consist

of 72.0%, 57.7%, and 39.8% DBI, respectively. The chemical structures of PDBIIs are summarized in Figure 1(d).

Thermal properties such as crystallization and glass transition are pivotal for dielectric elastomers. As shown in Figure 1(c), the PDBII and polyisoprene synthesized by redox emulsion polymerization are amorphous in the testing range of temperature, and the glass transition temperatures decreases with increasing isoprene content.

Effect of molar ratio of di-*n*-butyl to isoprene

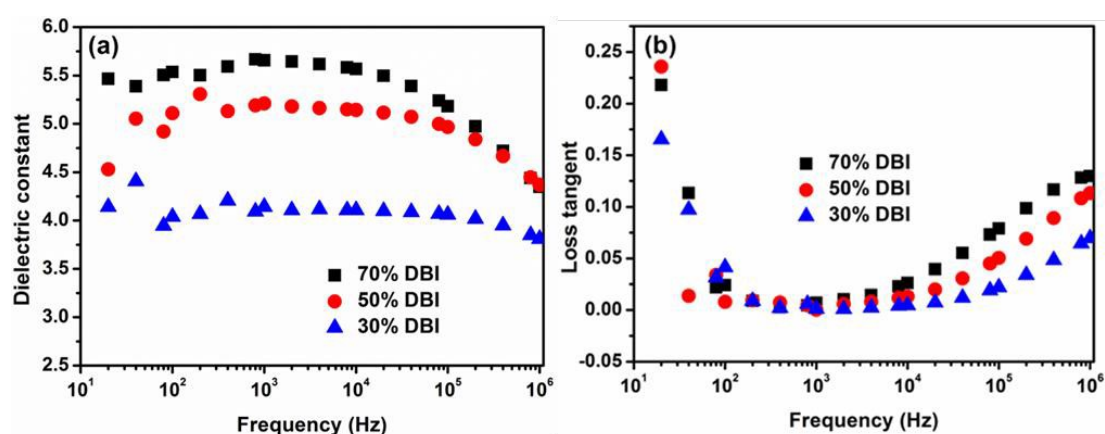


Figure 2. Frequency dependence of (a) dielectric constant and (b) loss tangent of crosslinked PDBII.

(70% DBI stands for 70% DBI in the feed.)

The curing characters of PDBIIs with different DBI content in the feed were listed in Figure S3 and Table S2. The frequency dependence of dielectric constant and loss tangent of crosslinked PDBII in the frequency range of 10 to 10^6 Hz is shown in Figure 2. The dielectric constant increases with increasing DBI content over the whole frequency range. As there are many polarizable ester groups on the side chains, DCP-crosslinked PDBII with 70% DBI exhibits a high dielectric constant of 5.6 at 10^3

Hz, which is higher than those of two commonly used dielectric elastomers: silicone elastomer (Nusil CF19-2186, 2.8)³ and acrylic elastomer (3M VHB, about 4.8)³. Generally, the more abundant the ester groups on the polymer side chain, the higher the dielectric constant of the polymer. The alkyl groups on the side chain always provide some plasticizing effect, but the amount of DBI on the polymer chain have to be optimized to guarantee a high elasticity. Thus, crosslinked PDBII with a DBI content of 70% will be selected in the following research.

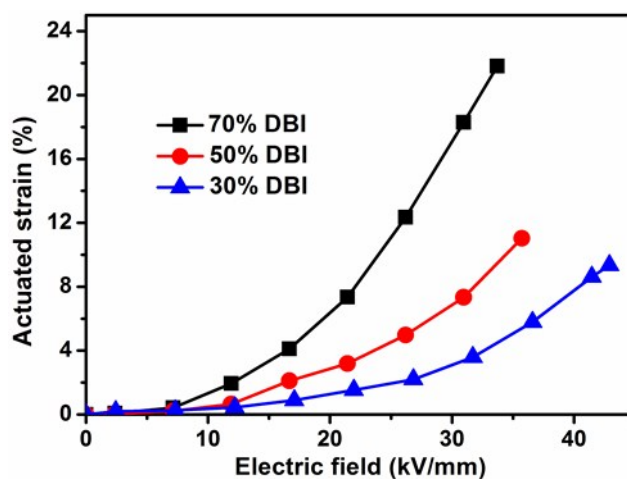


Figure 3. Actuated strain of crosslinked PDBII at different DBI contents.

The actuated strain of a dielectric elastomer under a given voltage is an important property. The actuated plane strain of PDBII as a function of applied electric field is shown in Figure 3. It can be seen that the actuated strain increases as the electric field increases. PDBII with 70% DBI displays a higher actuated strain than PDBII with 50% or 30% because the ester groups have strong polarity, which enhances the dielectric constant, and PDBII with 70% DBI has fewer double bonds and hence a lower crosslink density than PDBII with a lower DBI content.

Effect of crosslink density

The tensile strength, elastic modulus, electric breakdown strength, actuated strain, and response speed after stimulation are closely related to the crosslink density. Meanwhile, a high actuated strain at a low electric field is actively pursued. PDBII with a DBI content of 70%, crosslinked with different amounts of DCP, were further investigated. The Figure S4 shows that the PDBII is effectively crosslinked more than 1.5 phr of DCP in the PDBII matrix, and the optimum cure time were summarized in Table S3. And the torque at optimum cure time increases as the DCP dosage increases.

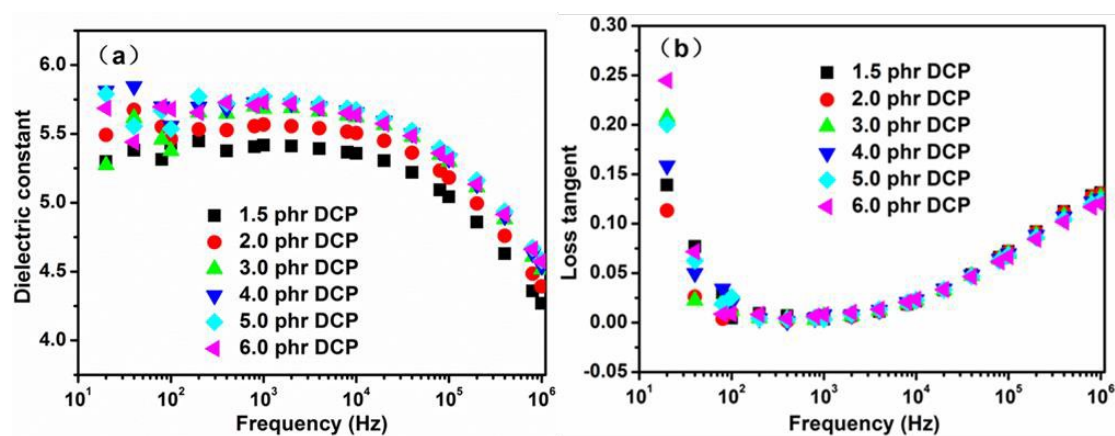


Figure 4. Frequency dependence of (a) dielectric constant and (b) loss tangent of PDBII (with 70% DBI) crosslinked by different amounts of DCP.

Figure 4(a) shows the frequency dependence of dielectric constant of PDBII at ambient temperature. With increasing DCP content, the dielectric constant first increases, probably because the free volume of the material decreases with increasing degree of crosslinking³⁶. However, the dielectric constant decreases with further increases of DCP dosage because a high crosslink density limits the polarization of the polymer chains. Meanwhile, the dielectric constant decreases significantly with increasing frequency at frequencies above 10^4 Hz because the polarization of the polymer chains do not have enough relaxation time to catch up with the frequency change of an applied electric field³⁷. Figure 4(b) shows that the crosslink density has

no significant effect on the loss tangent.

Figure 5 shows that the elongation at break decreases from 623% to 51% and the elastic modulus increases almost linearly from 0.092 MPa to 0.55 MPa with increasing DCP dosage. The modulus of crosslinked PDBII is of the same order of magnitude as two commercial dielectric elastomers: VHB 4910³⁸ (about 0.1 MPa) and DC 3481⁷ (Dow Corning SILASTIC 3481, about 0.35 MPa). With about the same elastic modulus, the PDBII dielectric elastomers can load about the same stress as the two commercial dielectric elastomers. However, further increases in elastic modulus will lead to a low driving factor for dielectric elastomer, which is defined as the ratio of dielectric constant to elastic modulus.

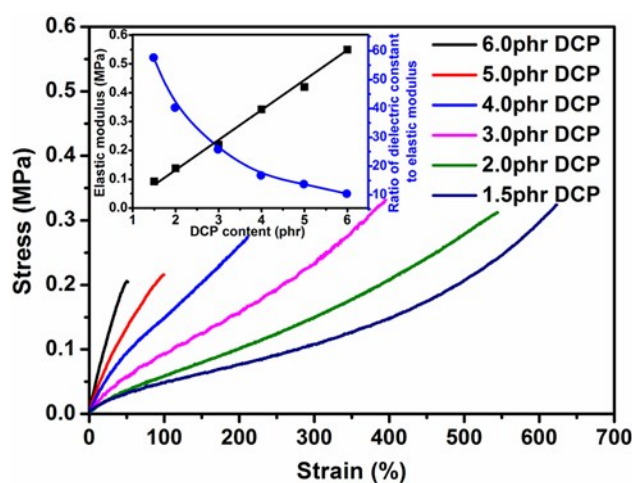


Figure 5. Stress-strain curves of PDBIIs (70% DBI) crosslinked by different contents of DCP and (inset) plots of elastic modulus versus DCP dosage and ratio of dielectric constant to elastic modulus versus DCP dosage.

The actuated strains of PDBIIs with different contents of DCP are shown in Figure 6. With decreasing DCP content, the actuated strain at a given electric field dramatically increases, mainly because a decrease in DCP content reduces the elastic modulus and

thus increases the ratio of dielectric constant to elastic modulus. The highest actuated strain at 20 kV/mm, 30 kV/mm, and 42 kV/mm are 14.7%, 20.0%, and 25.5%, respectively, without any prestrain. This actuated strain is relatively high compared with that of reported polymer dielectric materials under the condition of no prestrain (see supplementary information). However, the electric breakdown strength increases with increasing content of DCP, as shown in Figure 6(a), probably because of the decrease in sample defects with increasing DCP content.

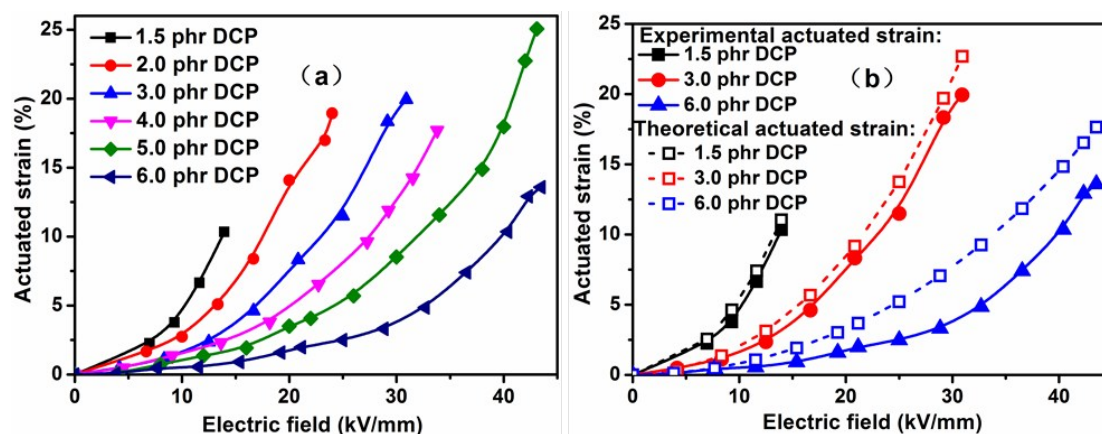


Figure 6. (a) Actuated strain of PDBII (70%DBI) crosslinked by different contents of DCP and (b) comparison between experimental and theoretical values of actuated strain.

Figure 6(b) compares the theoretical and experimental actuated strains of PDBII dielectric elastomer. The theoretical planar actuated strain S_p was calculated by equation (4). The theoretical values are higher than the experimental values under the same applied electric field. During the process of actuation, a small part of the electric energy is converted into thermal energy by mechanical loss and dielectric loss. The discrepancy between the experimental and theoretical values increases with increasing electric field because the mechanical loss increases as the actuated strain increasing and thus more electric energy is transformed into thermal energy, in agreement with

previous studies.^{39, 40}

BaTiO₃/PDBII composites

Figure 7 show the curing characteristics and stress-strain curves of BaTiO₃/PDBII composites. Usually, a polymer composite filled with inorganic nanoparticles has a higher elastic modulus and a lower elongation at break than the polymer matrix, and the elastic modulus increases and the elongation at break decreases with increasing filler content. The inorganic nanoparticles act as physical crosslinks in the polymer matrix to cause a reinforcing effect and hinder the mobility of polymer chains. However, as shown in Figure 7(b), the PDBIIs filled with 10 to 70 phr of BaTiO₃ have lower elastic modulus and higher elongation at break than the pure PDBII. Elastic modulus and curing character were summarized in Table S4. Similar results were first reported by Carpi¹⁴ for silicone dielectric elastomer filled with titanium dioxide. Furthermore, as the BaTiO₃ dosage increases to 90 phr, the elongation at break increases sharply to higher than 400% and the elastic modulus comes close to that at a BaTiO₃ dosage of 10 phr.

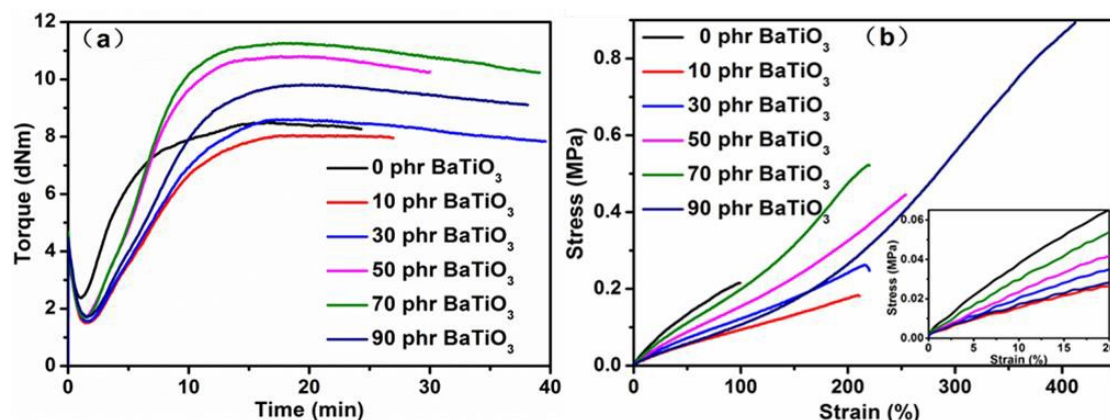


Figure 7. (a) Curing curves and (b) stress-strain curves of BaTiO₃-filled PDBIIs.

This unusual phenomena are mainly attributed to the decrease in crosslink density. The crosslink density can be illustrated by the torque increment (ΔS) between the maximum torque (S_{max}) and minimum torque (S_{min}) in the curing curve. The curing curves of PDBII elastomers with different dosage of BaTiO₃ are shown in Figure 7(a), and the data of S_{max} , S_{min} , ΔS , optimum cure time and elastic modulus are summarized in Table S4. As reported previously, the elastic modulus of BaTiO₃/PDBII is controlled by two factors: the softening effect as a result of reduced crosslinking and the hardening effect of the reinforcement of the filler network.⁴¹ Two mechanisms for the decrease in crosslink density in TiO₂-filled dielectric elastomers were proposed: polymer chain cleavage at the TiO₂ particles⁴² and the combination of the radicals produced by the TiO₂ particles with the radicals produced by DCP⁴¹. Although the pure PDBII presents the highest elastic modulus (see Figure 7(b)) as a result of high crosslink density, the torque of the filled PDBIIs (see Figure 7(a)) and the elastic modulus (see Figure 7(b)) increase as the BaTiO₃ dosage increases from 10 phr to 70 phr because of the filler hardening effect. The lower elastic modulus and higher elongation at break at 90 phr of BaTiO₃ than at lower dosages were probably due to secondary structures such as nanoparticle aggregates, which further hindered the crosslinking.

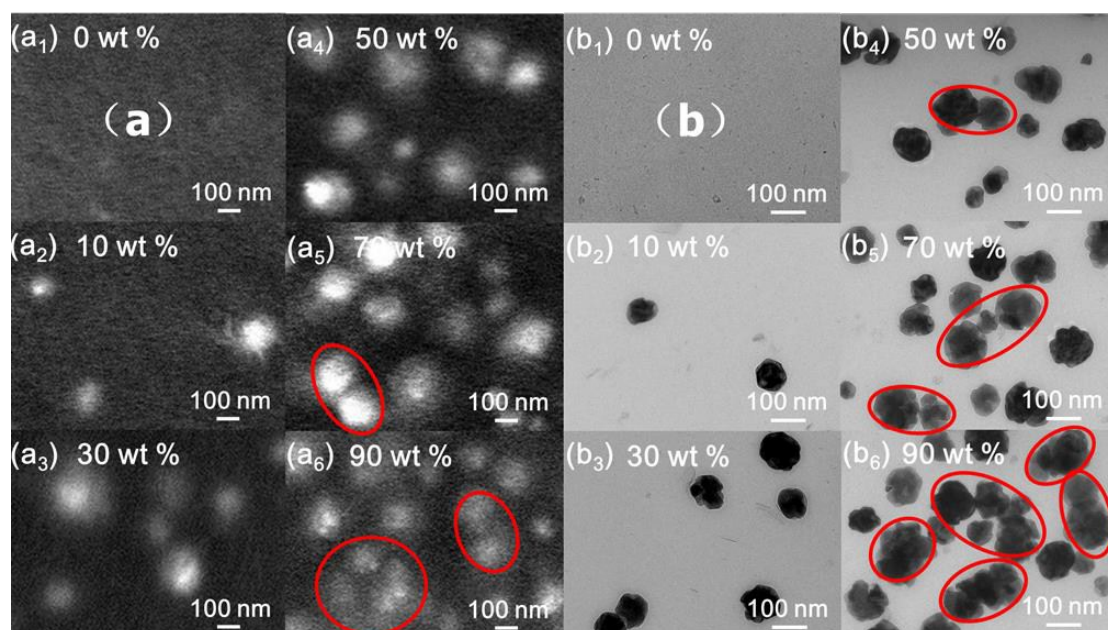


Figure 8. (a) Scanning electron microscope and (b) Transmission electron microscope micrographs of PDBII elastomers filled with different contents of BaTiO₃.

The Scanning electron microscope and Transmission electron microscope micrographs of BaTiO₃/PDBII composites are shown in Figures 8(a) and 8(b). The nanoparticles in the diameter range of 100-200 nm are uniformly dispersed in the PDBII matrix. However, the nanoparticle tended to aggregate even at only 10 phr. If the aggregates are sufficiently large and/or numerous, the particles will come into direct contact with one another to form agglomerates (circled in red)⁴³. An obvious filler network appears in Figure 8(b₆) for the composite with 90 wt % BaTiO₃, in which the crosslink reaction was most hindered.

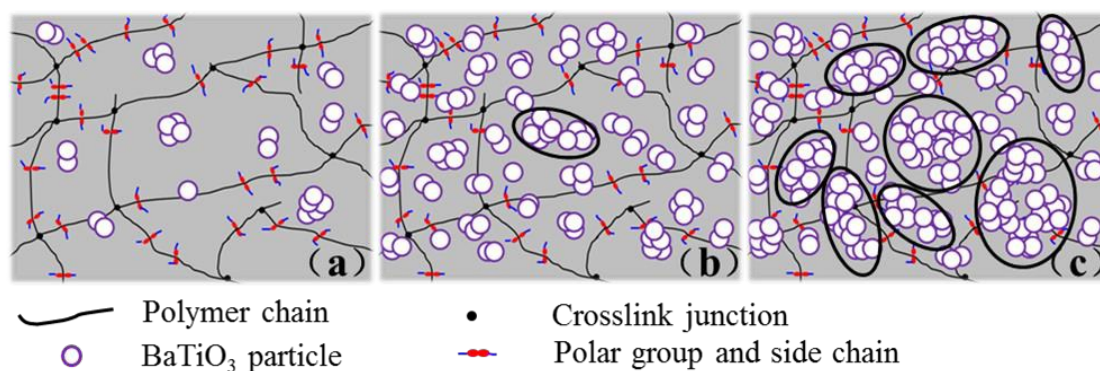


Figure 9. Schematic diagram of dispersion of different weight contents of BaTiO₃ in PDBII

elastomer: (a) 10 %, (b) 50%, and (c) 90%.

A simplified model of BaTiO₃/PDBII composites is shown in Figure 9. The high surface energy of BaTiO₃ nanoparticles results in strong physical adsorption and/or chemisorption, which make it easy for the nanoparticles to form aggregates. As a result, single particles are rare even at low contents of BaTiO₃, as shown in Figures 8(a₂), 8(b₂), and 9(a). As the BaTiO₃ content increases, secondary filler structures or filler network which may also be described as agglomerates are formed. However, filler networks on a macro scale are not formed until the BaTiO₃ exceeds the percolation threshold of 90 phr. Some polymer chains are trapped in the filler networks without being crosslinked. At moderate and high strains, uncrosslinked rubber is released from filler network as the agglomerates are destroyed, and acts as the polymer matrix. As a result, the elastic modulus of PDBII filled with 90 phr of BaTiO₃ decreases and the elongation at break increases sharply, as shown in Figure 7(b).

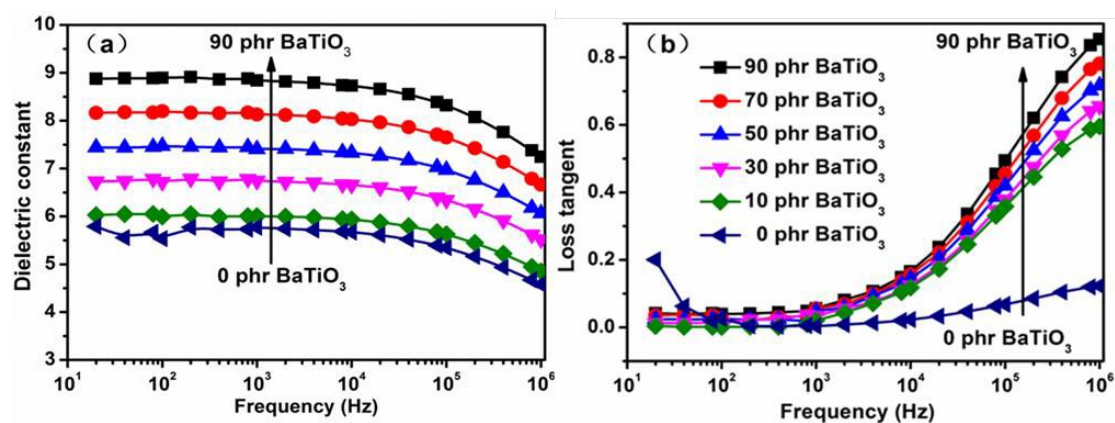


Figure 10. Frequency dependence of (a) dielectric constant and (b) loss tangent of BaTiO₃-filled PDBIIs.

Figure 10(a) shows the frequency dependence of the dielectric constant of BaTiO₃/PDBII elastomer composites with different contents of BaTiO₃. The dielectric constant increases with increasing content of BaTiO₃ particles at all frequencies because of the enhancement of electron polarization and interface polarization at the interface between the PDBII matrix and BaTiO₃ particles.⁴⁴ However, the electron polarization and interface polarization will increase not only the dielectric constant, but also the dielectric loss of the composites. Figure 10(b) shows the frequency dependence of the dielectric loss of the PDBII elastomer composites at room temperature. The dielectric loss of pure PDBII is smaller than those of all BaTiO₃/PDBII composites. As explained above, the semiconductor nature of BaTiO₃ is beneficial to the movement of electrical charge, leading to an increase in dielectric loss of BaTiO₃/PDBII composites. Besides, the dielectric loss of the composites increases rapidly with frequency at frequencies higher than 10⁴ Hz.

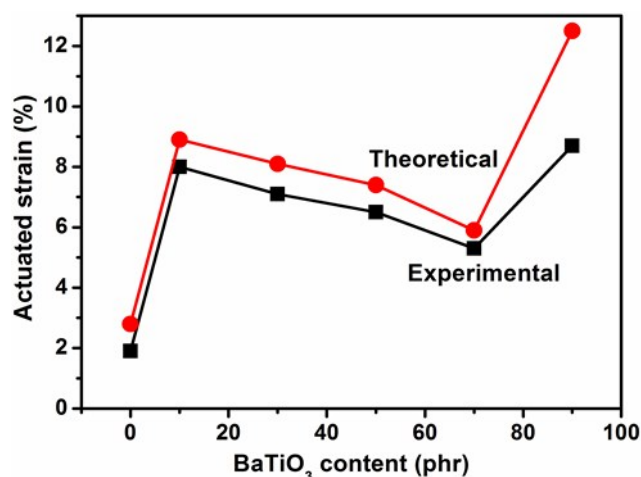


Figure 11. Comparison of theoretical (red dots) and experimental (black squares) actuated strains of BaTiO₃/PDBII composites at 15 kV/mm.

The theoretical and experimental actuated strains of PDBII elastomer composites with different contents of BaTiO₃ are plotted against the applied electric field Figure 11. There is a local maximum in actuated strain at an applied electric field of 15 kV min⁻¹ for the BaTiO₃/PDBII composite with 10 wt % of BaTiO₃. This local maximum in actuated strain of 8.0% was obtained without any prestrain and is 321% higher than the actuated strain of pure PDBII at the same applied electric field. An electric field of 29.2 kV/mm was needed to obtain almost the same actuated strain with pure PDBII elastomer; that is, a reduction of 48.6% in electric field was obtained with the composite. As the BaTiO₃ content increases from 10 wt % to 70 wt %, the actuated strain decreases because of a decrease in electromechanical sensitivity ($\beta = \epsilon_r/Y$). And the experimental data are in good agreement with theoretical predictions. However, the actuated strain increases sharply as the BaTiO₃ content increases from 70 wt % to 90 wt %, mainly because the decrease in elastic modulus discussed above. The discrepancy between experimental data and theoretical

prediction increases sharply because filler networks increase the conversion of electric energy to thermal energy through mechanical loss and dielectric loss.

Conclusion

The novel poly(di-*n*-butyl itaconate-*co*-isoprene) (PDBII) dielectric elastomer have been synthesized from itaconic acid, butanol, and isoprene by free radical redox emulsion polymerization. After being crosslinked by 3.0 phr of dicumyl peroxide (DCP), PDBII with a di-*n*-butyl itaconate content of 70%, a number-average molecular weight of 310,000, and a glass transition temperature of -38°C showed a permittivity of 5.68 at 10^3 Hz. The effect of DCP content on the mechanical, dielectric, and actuation properties was investigated. An actuated strain of 20% at an electric field of 30 kV mm^{-1} and an actuated strain of 25% at an electric field of 43 kV mm^{-1} were obtained with PDBIIs crosslinked with 3.0 and 5.0 phr of DCP, respectively, without any prestrain. PDBII (mass ratio of di-*n*-butyl itaconate to isoprene of 70/30) filled with 10.0 phr of barium titanate and crosslinked by 5.0 phr of dicumyl peroxide had an actuated strain of 8.0% at 15 kV mm^{-1} , 321% higher than the actuated strain of pure PDBII. This research may help establish a new and valuable route for dielectric elastomers.

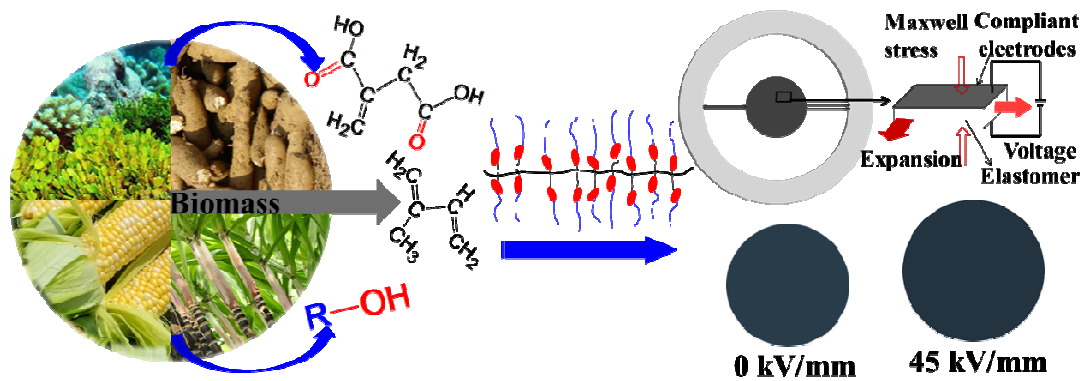
Acknowledgement

This work was supported by the National Natural Science Foundation of China (Grant Nos. 50933001, 51173007 and 51221002).

References

- 1 P. H. Vargantwar, A. E. Oezcam, T. K. Ghosh and R. J. Spontak, *Adv. Funct. Mater.* 2012, **22**, 100-2113.
- 2 Y. Jang and T. Hirai, *Soft Matter*, 2011, **7**, 10818-10823.
- 3 R. Pelrine, R. Kornbluh, Qibing Pei, Jose Joseph, *Science*, 2000, **287**, 836-839.
- 4 R. Kornbluh, R. Pelrine, Q. Pei, S. Oh and J. Joseph, *Proc. SPIE-Int. Soc. Opt. Eng.*, 2000, **3987**, 51-64.
- 5 P. Brochu and Q. Pei, *Macromol. Rapid Commun.*, 2010, **31**, 10-36.
- 6 F. Carpi, S. Bauer and D. De Rossi, *Science*, 2010, **330**, 1759-1761.
- 7 X. Q. Zhang, C. Lowe, M. Wissler, B. Jahne and G. Kovacs, *Adv. Eng. Mater.*, 2005, **7**, 361-367.
- 8 S. Chiba, M. Waki, R. Kornbluh and R. Pelrine, *Smart Mater. Struct.*, 2011, **20**, 124006.
- 9 M. Molberg, D. Crespy, P. Rupper, F. Nuesch, J. A. E. Manson, C. Loewe and D. M. Opris, *Adv. Funct. Mater.*, 2010, **20**, 3280-3291.
- 10 F. Carpi, G. Gallone, F. Galantini and D. De Rossi, *Adv. Funct. Mater.*, 2008, **18**, 235-241.
- 11 G. Gallone, F. Galantini and F. Carpi, *Polym. Int.*, 2010, **59**, 400-406.
- 12 K. H. Lee, J. Kao, S. S. Parizi, G. Caruntu and T. Xu, *Nanoscale*, 2014, **6**, 3526-3531.
- 13 G. Gallone, F. Carpi, D. De Rossi, G. Levita and A. Marchetti, *Mater. Sci. Eng., C-Biomimetic Supramol. Syst.*, 2007, **27**, 110-116.
- 14 F. Carpi and D. De Rossi, *IEEE Trans. Dielectr. Electr. Insul.*, 2005, **12**, 835-843.
- 15 D. Yang, L. Zhang, N. Ning, D. Li, Z. Wang, T. Nishi, K. Ito and M. Tian, *Rsc Adv.*, 2013, **3**, 21896-21904.
- 16 Y. Shen, Y. Lin, M. Li and C.-W. Nan, *Adv. Mater.*, 2007, **19**, 1418-1422.
- 17 J. K. Yuan, Z. M. Dang, S. H. Yao, J. W. Zha, T. Zhou, S. T. Li and J. Bai, *J. Mater. Chem.*, 2010, **20**, 2441-2447.
- 18 Z. M. Dang, L. Wang, Y. Yin, Q. Zhang and Q. Q. Lei, *Adv. Mater.*, 2007, **19**, 852-857.
- 19 K. Goswami, A. E. Daugaard and A. L. Skov, *RSC Adv.*, 2015, **5**, 12792-12799.
- 20 M. Tian, Z. Wei, X. Zan, L. Zhang, J. Zhang, Q. Ma, N. Ning and T. Nishi, *Compos. Sci. Technol.*, 2014, **99**, 37-44.
- 21 P. Kim, S. C. Jones, P. J. Hotchkiss, J. N. Haddock, B. Kippelen, S. R. Marder and J. W. Perry, *Adv. Mater.*, 2007, **19**, 1001-1005.
- 22 D. Yang, M. Tian, D. Li, W. Wang, F. Ge and L. Zhang, *J. Mater. Chem. A*, 2013, **1**, 12276-12284.
- 23 K. Hayashida, Y. Matsuoka and Y. Takatani, *RSC Adv.*, 2014, **4**, 33530-33536.
- 24 H. Stoyanov, M. Kolloosche, S. Risse, D. N. McCarthy and G. Kofod, *Soft Matter*, 2011, **7**, 194-202.
- 25 S. M. Ha, W. Yuan, Q. B. Pei, R. Pelrine and S. Stanford, *Adv. Mater.*, 2006, **18**, 887-891.
- 26 J. Cowie, I. McEwen and M. Y. Pedram, *Macromolecules*, 1983, **16**, 1151-1155.
- 27 J. Cowie, S. Henshall and I. McEwen, *Polymer*, 1977, **18**, 612-616.
- 28 J. Cowie, Z. Haq, I. McEwen and J. Velickovic, *Polymer*, 1981, **22**, 327-332.
- 29 V. Arrighi, I. McEwen and P. Holmes, *Macromolecules*, 2004, **37**, 6210-6218.
- 30 A. C. Genix and F. Lauprêtre, *Macromolecules*, 2006, **39**, 7313-7323.
- 31 A. C. Genix and F. Lauprêtre, *J. Non-Cryst. Solids*, 2006, **352**, 5035-5041.

- 32 V. Arrighi, A. Triolo, I. McEwen, P. Holmes, R. Triolo and H. Amenitsch, *Macromolecules*, 2000, **33**, 4989-4991.
- 33 W. J. Orts, K. M. Holtman and J. N. Seiber, *J. Agric. Food. Chem.*, 2008, **56**, 3892-3899.
- 34 R. Wang, J. Ma, X. Zhou, Z. Wang, H. Kang, L. Zhang, K. Hua and J. Kulig, *Macromolecules*, 2012, **45**, 4989-4991.
- 35 Z. Liu, Y. Han, C. Zhou, M. Zhang, W. Li, H. Zhang, F. Liu and W. J. Liu, *Ind. Eng. Chem. Res.*, 2010, **49**, 7152-7158.
- 36 G. Hougham, G. Tesoro and A. Viehbeck, *Macromolecules*, 1996, **29**, 3453-3456.
- 37 Z. M. Dang, H. P. Xu and H. Y. Wang, *Appl. Phys. Lett.*, 2007, **90**, 2901-12903.
- 38 D. Yang, M. Tian, H. Kang, Y. Dong, H. Liu, Y. Yu and L. Zhang, *Mater. Lett.*, 2012, **76**, 229-232.
- 39 H. Liu, L. Zhang, D. Yang, Y. Yu, L. Yao and M. Tian, *Soft Materials*, 2013, **11**, 363-370.
- 40 D. De Tommasi, G. Puglisi and G. Zurlo, *Appl. Phys. Lett.*, 2011, **98**, 125507-123509.
- 41 D. Yang, M. Tian, Y. Dong, H. Kang, D. Gong and L. Zhang, *J. Appl. Phys.*, 2013, **114**, 154104.
- 42 Y. M. Xu and C. H. Langford, *Langmuir*, 2001, **17**, 897-902.
- 43 Z. Wang, J. Liu, S. Wu, W. Wang and L. Zhang, *PCCP*, 2010, **12**, 3014-3030.
- 44 Z. M. Dang, Y. J. Xia, J. W. Zha, J. K. Yuan and J. Bai, *Mater. Lett.*, 2011, **65**, 3430-3432.



Design and preparation of bio-based dielectric elastomer with polar and plasticized sidechains showed high actuated strain at low electric field